British Journal of Pharmacology (2008) 155, 62–72

0007–1188/08 $30.00
www.brjpharmacol.org

RESEARCH PAPER

Bimodal effects of the K_v7 channel activator retigabine on vascular K^+ currents

SYM Yeung[1], M Schwake[2], V Pucovský[3] and IA Greenwood[1]

[1]*Division of Basic Medical Sciences, Ion Channels and Cell Signalling Research Centre, St George's University of London, London, UK;* [2]*Institute of Biochemistry, Christian-Albrechts University, Kiel, Germany and* [3]*Cardiovascular Biomedical Research Centre, School of Medicine and Dentistry, Queen's University Belfast, Belfast, UK*

Background and purpose: This study investigated the functional and electrophysiological effects of the K_v7 channel activator, retigabine, on murine portal vein smooth muscle.
Experimental approach: KCNQ gene expression was determined by reverse transcriptase polymerase chain reaction (RT-PCR) and immunocytochemical experiments. Whole cell voltage clamp and current clamp were performed on isolated myocytes from murine portal vein. Isometric tension recordings were performed on whole portal veins. K^+ currents generated by KCNQ4 and KCNQ5 expression were recorded by two-electrode voltage clamp in *Xenopus* oocytes.
Key results: KCNQ1, 4 and 5 were expressed in mRNA derived from murine portal vein, either as whole tissue or isolated myocytes. $K_v7.1$ and $K_v7.4$ proteins were identified in the cell membranes of myocytes by immunocytochemistry. Retigabine (2–20 μM) suppressed spontaneous contractions in whole portal veins, hyperpolarized the membrane potential and augmented potassium currents at −20 mV. At more depolarized potentials, retigabine and flupirtine, decreased potassium currents. Both effects of retigabine were prevented by prior application of the K_v7 blocker XE991 (10 μM). Recombinant KCNQ 4 or 5 channels were only activated by retigabine or flupirtine.
Conclusions and implications: The K_v7 channel activators retigabine and flupirtine have bimodal effects on vascular potassium currents, which are not seen with recombinant KCNQ channels. These results provide support for KCNQ4- or KCNQ5-encoded channels having an important functional impact in the vasculature.
British Journal of Pharmacology (2008) **155,** 62–72; doi:10.1038/bjp.2008.231; published online 9 June 2008

Keywords: KCNQ; K_v7; retigabine; XE991; vascular smooth muscle; RT-PCR; immunocytochemistry; isometric tension

Abbreviations: mPV, murine hepatic portal vein; PSS, physiological saline solution; RMP, resting membrane potential

Introduction

K_v7 ($K_v7.1$–$K_v7.5$) are a subfamily of voltage-gated K^+ channels encoded by the *KCNQ* genes. Each K_v7 protein has a particular distribution with $K_v7.1$ expressed predominantly by cardiac myocytes, whereas $K_v7.2$–7.5 are considered 'neuronal' (Jentsch, 2000; Schroeder *et al*., 2000) and $K_v7.4$ having a specialized cellular location in auditory neurons (Kharkovets *et al*., 2000). These K^+ channels are essential regulators of cardiac and neuronal action potentials as emphasized by the fact that mutations in their genes underlie a number of clinical symptoms. Most notably mutations in $K_v7.1$ result in cardiac arrhythmias; mutations in $K_v7.2$ and $K_v7.3$ result in neuronal excitability and underlie benign neonatal familial epilepsy (Jentsch, 2000); whereas a mutation in $K_v7.4$ results in hereditary deafness (Kubisch *et al*., 1999).

Correspondence: Dr IA Greenwood, Division of Basic Medical Sciences, St George's University of London, Cranmer Terrace, London SW17 0RE, UK.
E-mail: i.greenwood@sgul.ac.uk
Received 6 March 2008; revised 14 April 2008; accepted 24 April 2008; published online 9 June 2008

The study of K_v7 channels has largely relied on the use of the blockers such as linopirdine and XE991, but these compounds do not discriminate between the five K_v7 isoforms. Recently the anti-convulsant retigabine (D23129, *N*-(2-amino-4-(4-flurobenzylamino)-phenyl)carbamic acid ethyl ester)) has been shown to augment heteromers of $K_v7.2$ and $K_v7.3$ (Main *et al*., 2000; Wickenden *et al*., 2000), which underlie the neuronal M-current (Wang *et al*., 1998). Retigabine has now been shown to activate all neuronal K_v7 channels (that is $K_v7.2$–7.5) but does not affect $K_v7.1$ in concentrations up to 100 μM (Tatulian *et al*., 2001; Schenzer *et al*., 2005; Wuttke *et al*., 2005). There are numerous studies on the pharmacology of K_v7 channels in expression systems but fewer using native preparations (Tatulian *et al*., 2001). Even less data are available on K_v7 channels in smooth muscle cells where these genes have recently been identified (Ohya *et al*., 2003; Yeung and Greenwood, 2005; Brueggemann *et al*., 2006; Yeung *et al*., 2007). The present investigation analyses the effects of retigabine on the native K^+ currents in murine hepatic portal vein (mPV) myocytes,

where the effects of the K_v7 channel inhibitor XE991 have been characterized extensively (Yeung and Greenwood, 2005). This study provides the first description of retigabine effects on endogenous K^+ currents in a non-neuronal cell type. Furthermore, these data give some insight into the molecular identity of the native K_v7 channel in these vascular smooth muscle cells.

Materials and methods

Conventional isometric tension recordings

All experiments were performed on portal veins from BALB/c mice (6–8 weeks) killed by schedule 1 methods, in accordance with the UK Animals Act. Isometric tension recordings on whole mPV were performed as described in Yeung and Greenwood (2005). Briefly, the portal vein was removed from the animal and all connective tissue and fat were removed. The mPV was placed into a 10 mL organ bath containing Krebs solution aerated with 95% O_2/5% O_2 and maintained at 37 °C then set to a resting tension of 0.1 g. Changes in tension were recorded using BIOPAC Systems Inc. force transducer and AcqKnowledge software (version 3.7) sampling at 2.5 kHz. All veins exhibited spontaneous activity within minutes of being set up and this activity was maintained for the duration of the experiment (Yeung and Greenwood, 2005). To quantify the data, a single contraction was defined as an increase in tension from the baseline that was separated from another contraction by a period at the basal tension of at least 1 s. Intercontraction interval was taken as the period between two peaks of individual contractions. Contraction duration was taken as the total time that the tension remained above 10% of the maximal contraction.

Cell dissociation

Single smooth muscle cells were isolated enzymatically from mPV before each experiment using the protocol described by Yeung and Greenwood (2005). This procedure involved treating tissues with 100 μM Ca^{2+} physiological saline solution (PSS) containing 0.3 mg mL^{-1} protease (type XIV, Sigma, UK); then with 0.6 mg mL^{-1} collagenase (type I, Calbiochem, UK) for 6 min each. Dispersed cells were kept on ice until required.

RNA extraction and reverse transcription-PCR

The mPV was excised from the animal and placed immediately into RNA later (Ambion, UK). All extraneous tissue was removed and the mPV was cut into smaller pieces and placed into lysis buffer containing β-mercaptoethanol. Total RNA was extracted from the tissues using spin column technology (RNeasy kits, Qiagen, UK) according to the manufacturer's protocol and incorporating an initial 10 min incubation with proteinase K. RNA was finally eluted with water and quantified using the NanoDrop spectrophotomer (ND-1000, NanoDrop Technologies, UK). Total RNA from murine heart and brain were extracted in the same manner and were subsequently used as positive controls. 100 ng total RNA was reverse transcribed using the reverse transcriptase enzyme MMLV (Invitrogen, UK). All samples had a respective RT-control, that is, no MMLV was put into the sample. PCRs used outer primers designed specifically to detect KCNQ1–5 (Yeung *et al*., 2007). All reactions were performed with an initial denaturation step at 94 °C for 2 min, followed by 35 cycles at 94 °C for 30 s, annealing temperature for 30 s and 72 °C for 1 min. The reaction was completed with a final extension step at 72 °C for 10 min. For nested PCRs a primary PCR using outer primers and 25 cycles was employed. This product was further amplified by a secondary 35 cycle PCR using inner primers (mKCNQ1, forward: 5′-CCATCATTGA CCTCATCGTG-3′, reverse: 5′-GGCGAAGACAGAGAAACA GG-3′; mKCNQ2, forward: 5′-AGGAAGCCGTTCTGTGTGA T-3′, reverse: 5′-GCAGAGGAAGCCAATGTACC-3′; mKCNQ3, forward: 5′-AAGACAGGGGCTATGGGAAT-3′, reverse: 5′-TTT TGGAGTGGATGGAGGTC-3′; mKCNQ4, forward: 5′-GAGCA GTATTCAGCAGGACA-3′, reverse: 5′-AGTAGAAGCCCAGCA GCAGA-3′; mKCNQ5, forward: 5′-CGCCAGAAGCATTTTGA GA-3′, reverse: 5′-TGGGAACTCTTGAGCCGTAG-3′). All reactions were carried out using a Touchgene thermal cycler (Techne, UK). All PCR products were sequenced using the ABC Sequencing Service at Imperial College London.

Immunocytochemistry

Single cells were fixed and stained for confocal microscopy as described previously (Saleh *et al*., 2005; Yeung *et al*., 2007). Protein expression was identified by immunofluorescence using antibody against $K_v7.1$ (Alomone Laboratories, Israel, 1:600 dilution), two against $K_v7.4$ (Kv7.4SC from Santa Cruz Biotechnology, USA, 1:200 dilution) and $K_v7.4$J (raised against a different epitope and kindly provided by T Jentsch, 1:50 dilution, Kharkovets *et al*., 2000). The labelling was visualized with Alexa Fluor 488-conjugated chicken anti-rabbit antibodies (1:500), Alexa Fluor 633-conjugated donkey anti-goat antibodies (1:500) or Alexa Fluor 488-conjugated donkey anti-goat antibodies (1:500).

Confocal microscopy

The cells were imaged using a Zeiss LSM 510 laser scanning confocal microscope (Carl Zeiss, Germany). The excitation beam was produced by either argon (488 nm) or helium-neon (633 nm) laser and delivered to the specimen through a Zeiss Apochromat 63 × oil immersion objective (numerical aperture 1.4). Emitted fluorescence was captured using LSM 510 software (release 3.2, Carl Zeiss, Germany).

Analysis of images

An image cutting horizontally through approximately the middle of the cell was selected out of a z-stack of images. To assess the cellular distribution of K_v7 channels a circular area of 0.78 μm^2 (diameter approx. 1.0 μm; referred to as Region 1) was randomly selected in the subplasmalemmal area of the cell (Figure 7bi). Another circular area of 0.78 μm^2 (Region 2) was selected so that the perimeter of such circle touched the perimeter of Region 1 and the line going through the centre of these circles was perpendicular to the edge of the cell, thought to be the plasma membrane.

A percentage of fluorescing pixels (%FP) was calculated in both Regions using the formula:

$$\%FP = 100 \times \frac{n(p > \text{threshold})}{n(p)},$$

where $n(p > \text{threshold})$ is the number of pixels within the Region whose intensity equalled or exceeded the threshold value (one s.d. of the pixel intensity) and $n(p)$ the total number of pixels in the Region. The % FP values were then compared with each other and with the % FP in the whole confocal plane of the cell.

The average pixel fluorescence (APF) value was used to compare the overall fluorescence signal between the staining and its controls and was calculated using the formula:

$$APF = \frac{\sum i(p)}{n(p)} (\text{I.U./pixel}),$$

where $i(p)$ is the intensity of a pixel within the confocal plane of the cell and $n(p)$ is the total number of pixels of the plane. Statistical evaluation and graphs were done using MicroCal Origin software (MicroCal Software Inc., USA) and final images were produced using CorelDraw 10 software (Corel Corporation, Canada).

Current and voltage recordings

Whole cell currents were recorded at room temperature (20–22 °C) using the conventional, ruptured-patch configuration of the whole cell technique with internal and external solutions as described in Yeung and Greenwood (2005). Cells were allowed to equilibrate for 5 min following establishment of the recording, then a current voltage protocol from −100 to +60 mV was run (500 ms per step, 20 mV increments) from a holding potential of −60 mV. After this procedure, the cell was stepped to −20 mV for 500 ms every 20 s whereupon different agents were applied. Current voltage protocols were run once the effect of a certain drug had stabilized. Membrane potential recordings were made using the current clamp setting on the amplifier with the perforated patch variant of the whole cell recording configuration. Amphotericin (300 μg mL^{-1}) was included in the pipette solution in such cases and recordings commenced when the series resistance was <40 MΩ. All recordings were sampled at 5 kHz and low-pass filtered at 2 kHz. Results are expressed as mean ± s.e.mean and n as the number of cells. Statistical analyses were performed using Student's t-test and were considered significant at the $P<0.05$ level.

Expression in Xenopus laevis oocytes

Starting from KCNQ1, KCNQ4 and KCNQ5 cDNAs, which were subcloned into expression vector pTLN, capped RNA was transcribed using SP6 RNA polymerase in mMessage mMachine kit (Ambion, Austin) after linearization of the cDNA with *HpaI*. Individual stage V to VI oocytes were obtained from anaesthetized frogs and isolated by collagenase treatment. 10 ng of total KCNQ cRNA were injected into oocytes. Following injection, oocytes were kept at 17 °C in ND96 solution (96 mM NaCl, 2 mM KCl, 1.8 mM $CaCl_2$, 1 mM $MgCl_2$, 5 mM HEPES, pH 7.4).

Two-electrode voltage clamp electrophysiology

Two to three days after injection two-electrode voltage clamp measurements were performed at room temperature in ND96 using an npi Turbotec amplifier (npi electronics, Tamm, Germany) and pClamp9 software (Axon Instruments, Union City, CA, USA). For experiments examining the effect of retigabine or flupirtine, 1, 10, or 100 μM of retigabine or flupirtine was added to ND96 from a 100 mM stock solution, which was prepared in DMSO and kept at 4 °C in the dark.

Drugs and solutions

PSS contained (in mM): NaCl (125), KCl (5.4), $NaHCO_3$ (15.4), Na_2PO_4 (0.33), KH_2PO_4 (0.34), glucose (10) and HEPES (11), adjusted to pH 7.4 with NaOH. The external solution contained (in mM) NaCl (126), KCl (5), $MgCl_2$ (1), $CaCl_2$ (0.1), glucose (11) and HEPES (10), adjusted to pH 7.2 with NaOH. For current clamp experiments, $CaCl_2$ was raised to 2.5 mM. The internal solution contained (in mM): KCl (130), $MgCl_2$ (1), ATP (Na^+ salt, 3), GTP (0.1), HEPES (10), EGTA (5), adjusted to pH 7.2 with KOH. The Krebs solution for the functional experiments contained (in mM): NaCl (125), KCl (4.6), $CaCl_2$ (2.5), $NaHCO_3$ (15.4), Na_2PO_4 (1), $MgSO_4$ (0.6) and glucose (10). XE991 and flupirtine were purchased from Ascent Scientific (Weston-super-Mare, UK) and Sigma Chemical Company (Poole, Dorset, UK), respectively. All drugs were made up as a 100 mM stock with dimethyl sulphoxide (DMSO) and frozen as small aliquots. Channel and gene terminology conforms to the BJP Guide to Receptors and Channels (Alexander *et al*., 2008).

Results

Retigabine decreases mPV contractility

Previous isometric tension experiments showed that retigabine, and a structurally similar compound flupirtine, relaxed pre-contracted segments of murine aorta and conduit artery (Yeung *et al*., 2007). In this study, isometric tension recordings were undertaken to see whether retigabine had a similar functional effect in whole mPV. Under control conditions, all samples exhibited spontaneous rhythmic contractile activity with various patterns (Figure 1; also Yeung and Greenwood, 2005). Application of 20 μM retigabine rapidly affected contractile activity (Figure 1), manifested as a marked decrease in the amplitude of individual contractions (74.2 ± 3.7%, $P<0.01$, $n=4$). A similar inhibitory effect was observed with 3 μM retigabine, which decreased the amplitude of individual contractions from 0.0075 ± 0.0003 g to 0.0035 ± 0.00015 g ($P<0.01$, $n=3$). The inhibitory effect of retigabine was readily reversed upon washout (Figure 1). In contrast to its effects on spontaneous activity, 20 μM retigabine had no effect on tonic contractions produced by 60 mM KCl, which were 0.21 ± 0.02 g and 0.19 ± 0.02 g ($n=4$) in the absence and presence of retigabine. These data showed that retigabine had a spasmolytic

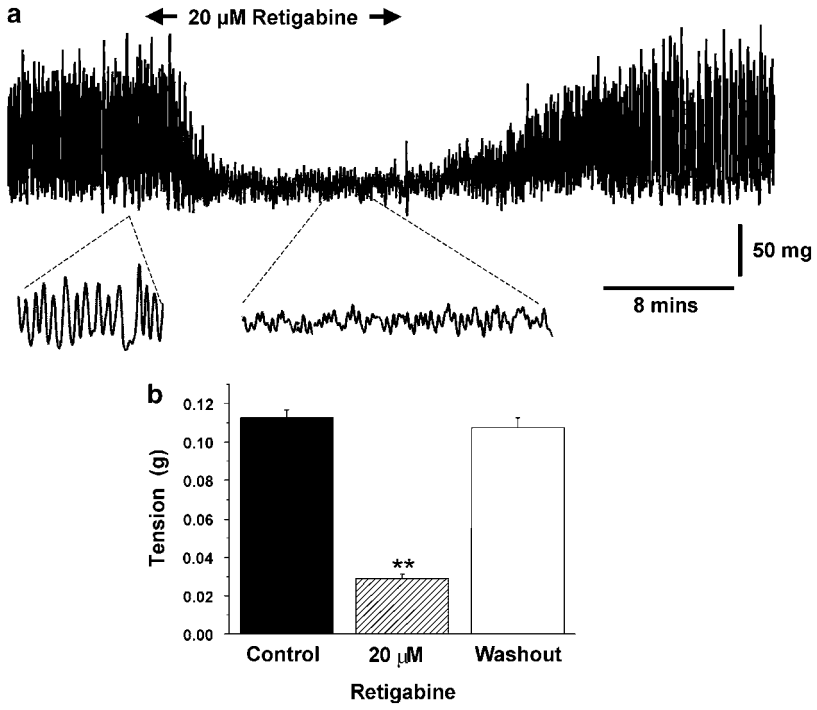

Figure 1 Retigabine inhibits excitability of whole mPV tissue. (**a**) Example of isometric tension recording in the absence and presence of 20 μM retigabine. Lower traces show magnifications of the sections highlighted. (**b**) Bar chart shows mean tension in the absence (solid bars) and presence of retigabine (hatched bars) and upon washout (open bars). ** denotes statistical significance retigabine versus control at $P<0.01$.

effect in whole mPV that was not due to the direct blockade of voltage-dependent calcium channels.

Retigabine hyperpolarizes the resting membrane potential

Current clamp recordings were made using the amphotericin -perforated patch configuration to see the effect of retigabine on membrane potential. In these cells the mean resting membrane potential (RMP) was -44.2 ± 2 mV ($n=7$). In each cell spontaneous changes in membrane potential were apparent (Figure 2). Spontaneous depolarizations ranged in amplitude between 3 and 17 mV (mean $= 12 \pm 1$, $n=7$ cells) and occasionally these depolarizations generated an overshooting action potential. Spontaneous hyperpolarizations were also apparent in all cells (Figure 2). Application of 3 and 10 μM retigabine hyperpolarized the RMP by 5.5 ± 0.9 and 8.9 ± 1.3 mV, respectively (Figure 2, $n=5$ & 6). Retigabine also prevented the generation of spontaneous depolarizations. Interestingly, in one cell where no change in membrane hyperpolarization was apparent after application of 3 μM retigabine, spontaneous depolarizations were still abolished. These data show that retigabine effectively suppressed membrane excitability in mPV myocytes.

Retigabine activates K^+ current in mPV

Experiments were undertaken to assess whether the functional effect of retigabine were mediated by an increase in K^+ current, as observed in neurones. Application of 1 μM retigabine, produced an increase in current at −20 mV in two of five cells tested (mean increase was 39 pA) whereas 3 μM retigabine markedly enhanced currents recorded at −20 mV in all cells tested (see Figure 3ai for example). The mean retigabine-sensitive current (exemplified by Figure 3aii) was 77 ± 16 pA ($n=6$). Application of 10 μM retigabine produced an augmentation at −20 mV in all cells tested (mean-48 ± 12 pA, $n=9$) whereas 20 μM retigabine produced an enhancement in 14 out of 17 cells tested (mean increase was 59 ± 12 pA). These effects of retigabine were not voltage-dependent in the physiological voltage range (from −60 to −20 mV, Figure 3b) and was associated with a small, leftward shift of the voltage-dependence for activation (data not shown, $\Delta V_{\frac{1}{2}}$: 3 μM = 13 ± 3 mV ($n=5$), 10 μM = 11 ± 2 mV ($n=5$), 20 μM = 11 ± 2 mV ($n=12$)). Flupirtine, a structural analogue of retigabine also augmented currents with a mean increase at −20 mV of 41 ± 11 pA ($n=4$) produced by 30 μM flupirtine. These data represent the first recording of retigabine and flupirtine effects on endogenous K^+ currents from any type of smooth muscle cell.

When the voltage range was extended to more positive potentials, a marked inhibition of currents by retigabine was apparent. The peak and steady state currents at 0 mV, +20 mV and +40 mV (Figure 4ai) were clearly diminished in the presence of 20 μM retigabine (Figure 4aii). This inhibition was reversed upon washout and therefore does not represent current rundown. The inhibitory effect of retigabine is highlighted when the retigabine-sensitive currents at these test potentials are calculated, as shown in Figure 4b. The simultaneous stimulation and inhibition of K^+ currents by retigabine resulted in the appearance of a 'bell' shaped current–voltage relationship for the retigabine-sensitive current (Figure 4c). Moreover, the potential at which inhibition was recorded was dependent on the concentration of retigabine. Thus, at +20 mV the current

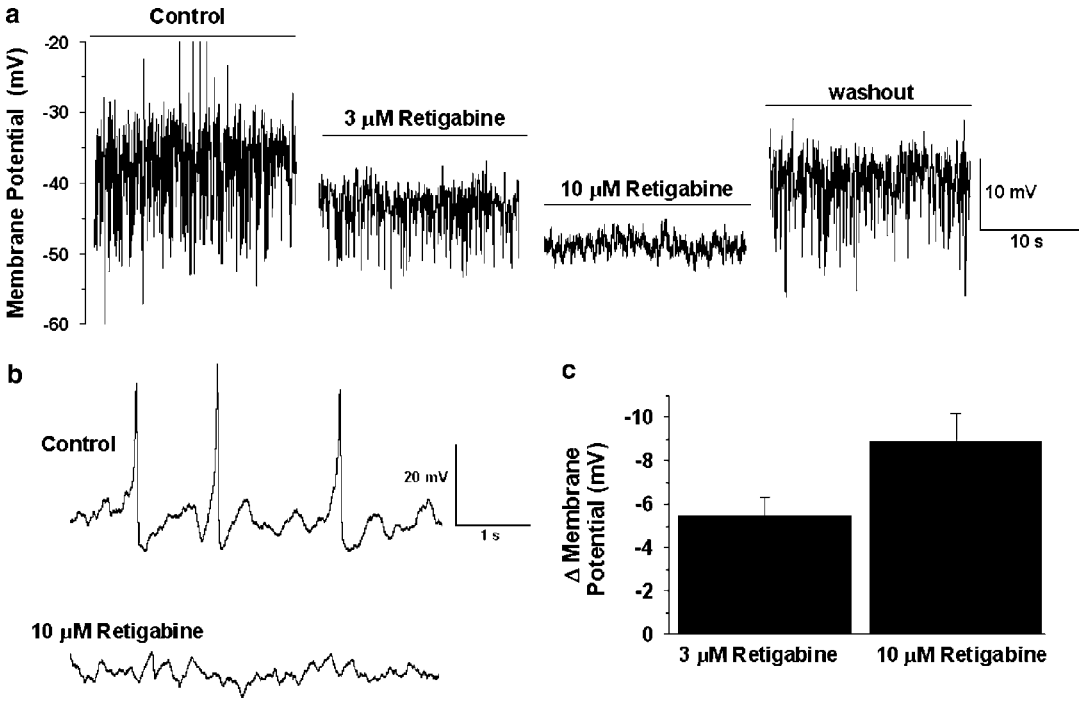

Figure 2 Effect of retigabine on membrane potential recordings in current clamp mode. (**a**) Example of membrane potential in the absence and presence of retigabine. Each panel shows a 20 s sample of membrane potential recording either in the absence of retigabine or after 5 min application of 3 μM and then 10 μM retigabine. Right panel shows the membrane potential 7 min after washout of retigabine. Upward and downward deflections denote spontaneous depolarizations and hyperpolarizations. (**b**) shows an amplified view of membrane potential recordings in the absence and presence of 10 μM retigabine showing the lack of spontaneous membrane depolarizations in the presence of this agent. Panel (**c**) shows the mean membrane hyperpolarization produced by 3 and 10 μM retigabine ($n = 5$ and 6, respectively).

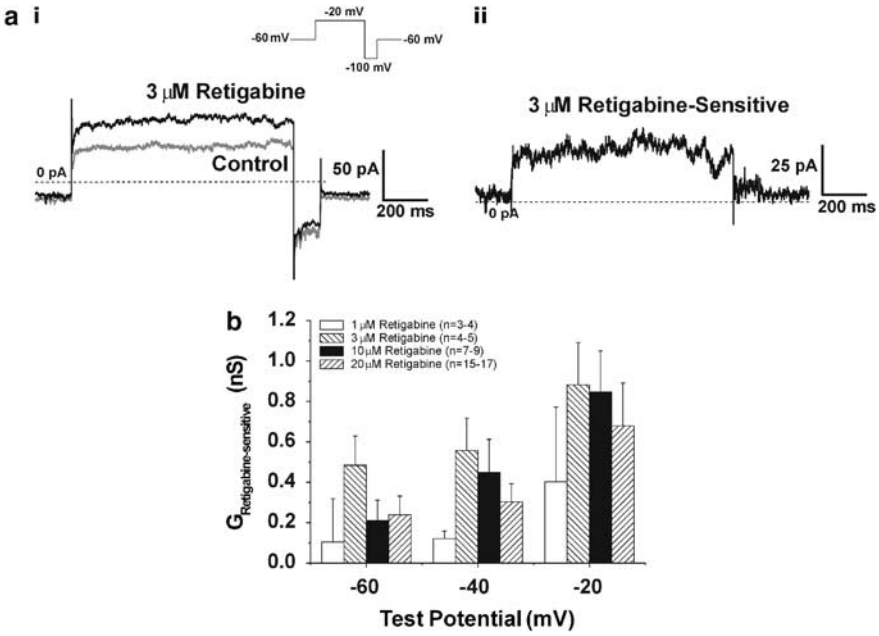

Figure 3 Activation of K^+ currents by different concentrations of retigabine. Panel (**ai**) shows currents evoked by stepping from −60 to −20 mV in the absence and presence of 3 μM retigabine. (**aii**) shows the retigabine-sensitive current from (**ai**). (**b**) shows the effect of a range of retigabine concentrations on K^+ conductance (I/V-Vr) at −60, −40 and −20 mV.

was decreased by 78 ± 33 pA ($n = 13$) and 68 ± 24 pA ($n = 4$) by 20 and 10 μM retigabine, respectively but was increased by 26 ± 42 pA ($n = 5$) by 3 μM retigabine. This led to a rightward shift in the threshold potential for current inhibition from ∼−5 mV for 20 μM retigabine to ∼+25 mV for 3 μM retigabine (see Figure 4c). Furthermore, there was no

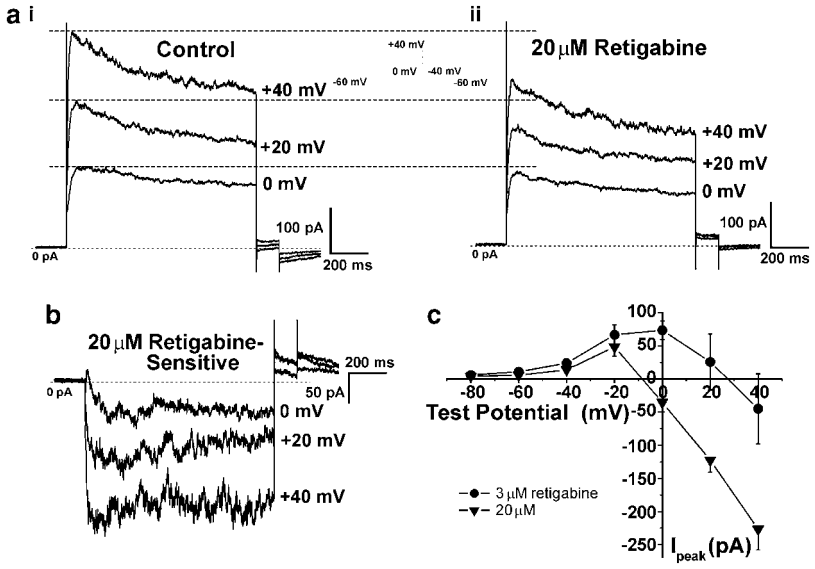

Figure 4 Retigabine inhibited the K^+ currents at positive potentials in a concentration-dependent manner. Current recordings at 0, +20 and +40 mV in the (**ai**) absence and (**aii**) presence of 20 μM retigabine. (**b**) Currents sensitive to retigabine at these potentials. (**c**) Current–voltage plot of peak current amplitudes sensitive to 3 and 20 μM retigabine.

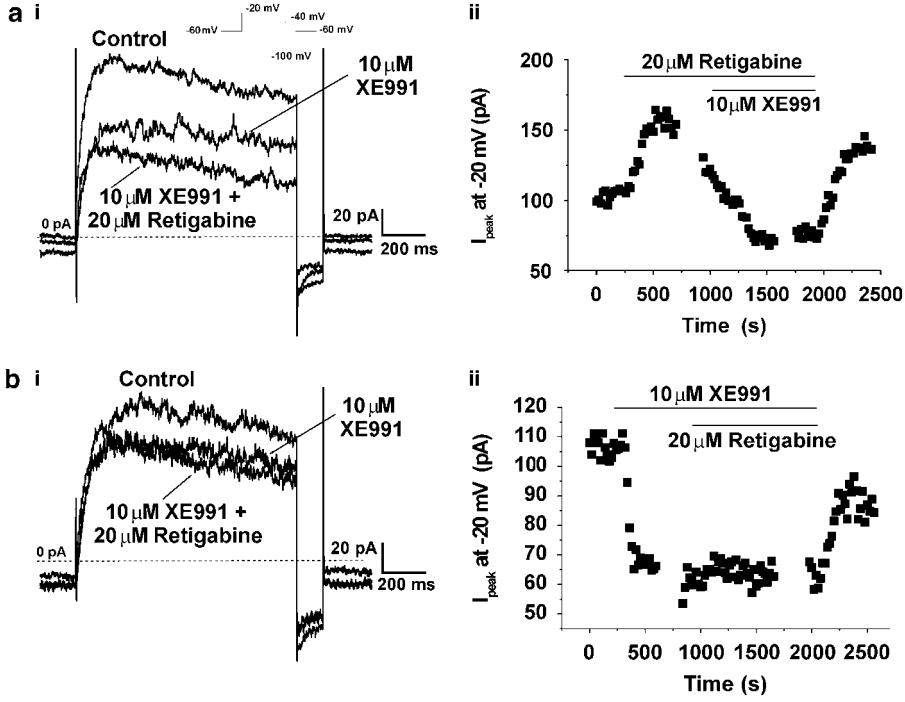

Figure 5 The effects of retigabine were sensitive to XE991. Panel (**ai**) show currents at −20 mV in the presence of retigabine and the subsequent application of XE991. (**aii**) shows the amplitude of currents at −20 mV over time for the experiment in (**ai**). (**bi**) shows the lack of effect of retigabine on currents at −20 mV in a cell bathed in 10 μM XE991. (**bii**) shows the amplitude of currents at −20 mV over time for the experiment in (**bi**).

correlation between the amount of current increase at −20 mV and the degree of inhibition at +40 mV ($R^2 = 0.1$). Flupirtine also inhibited K^+ currents at positive potentials with a mean decrease produced by 30 μM flupirtine at +40 mV of 23 ± 7 pA (data not shown, $n = 4$). These data show that retigabine and flupirtine have bimodal effects on endogenous K^+ currents, which are manifest at different potentials.

Retigabine-induced effects are sensitive to blockade of K_v7 channels by XE991

Experiments were instigated to ascertain whether the stimulatory effects of retigabine were sensitive to low concentrations of the K_v7 blocker XE991 (Wang *et al.*, 2000; Yeung and Greenwood, 2005) and therefore mediated by K_v7 channels. As Figures 5ai and 5aii show, the current recorded in the presence of retigabine (20 μM) was inhibited

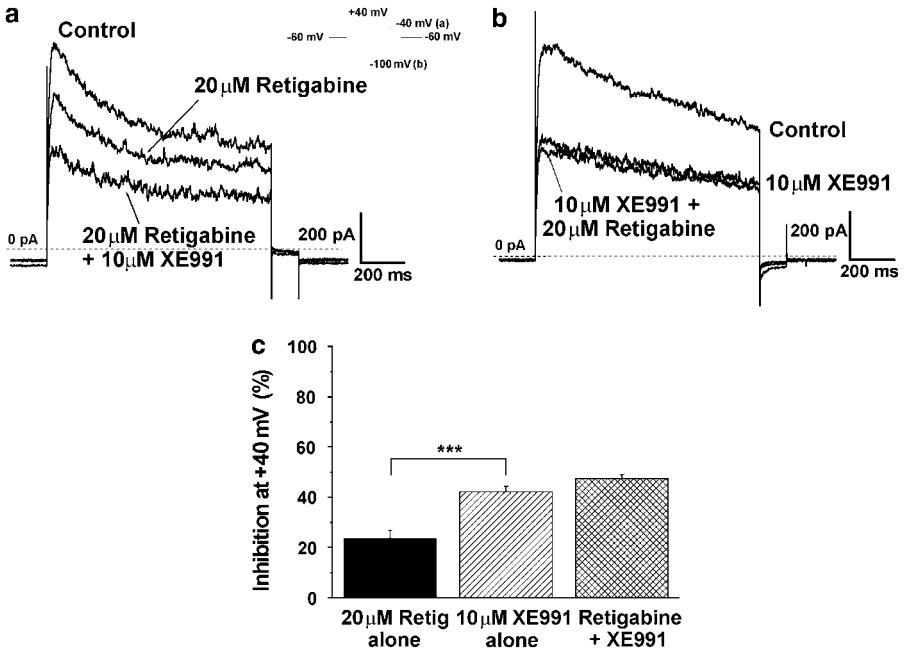

Figure 6 The inhibitory effects of retigabine and XE991 were not additive. Current recordings at V_T +40 mV with (**a**) retigabine alone followed by retigabine with added XE991. The inhibition by 10 μM XE991 alone (**b**) was not altered when retigabine was added. (**c**) Histogram shows mean ± s.e.m. (all $n=7$) block of mPV current (***$P<0.001$).

by 10 μM XE991. The mean inhibition produced by 10 μM XE991 was 78.4 ± 5.1% ($n=3$) and 64.5 ± 11.0% ($n=9$) for cells bathed in 3 and 20 μM retigabine respectively. As Figure 5bi and the time course (Figure 5bii) show pre-treatment with 10 μM XE991 prevented the stimulatory effect of retigabine at negative potentials (representative of five such experiments). As the outward currents produced by membrane depolarization of PV myocytes represent the net product of many different types of channels, the inhibition produced by retigabine at positive potentials might reflect a bimodal effect on K_v7 channels or an additional effect on a different K^+ channel. Consequently, studies were undertaken to determine if the inhibitory effect of retigabine was additive to that of XE991. Figure 6 shows current recordings from two different cells isolated from the same animal (a, b). At V_T +40 mV 20 μM retigabine alone (panel a) inhibited the peak outward current by 29%. Further block was observed with the addition of 10 μM XE991 with peak outward current being reduced in total by 48% in this cell. In the other cell (panel b), 10 μM XE991 alone (panel b) blocked peak outward current amplitude by 44% and no further inhibition was observed when retigabine was added. Mean data for nine such experiments are presented in the histogram (panel c) which shows that the inhibition produced by retigabine alone was significantly less ($P<0.001$) than XE991 but the cumulative effect of XE991 and retigabine was not significantly different from the effect of XE991 alone. These data suggest both the activator retigabine and blocker XE991 exert their effects on the same channel protein. In contrast, pre-application of the selective $K_v7.1$ channel blocker chromanol 293B (30 μM, Lerche *et al*., 2007), which reduced currents at +40 mV by 350 ± 54 pA ($n=5$), did not prevent the retigabine-induced inhibition at this potential. Thus, the mean decrease in current at +40 mV produced by 10 μM retigabine in the presence of chromanol 293B was 120 ± 36 pA ($n=5$), which was similar to the inhibition produced by 10 μM retigabine in the absence of chromanol (152 ± 13 pA, $n=6$).

mPV myocytes express KCNQ4 mRNA and $K_v7.4$ protein

Figure 7ai shows that mRNA for KCNQ1 and KCNQ4 was detected by RT-PCR in mPV tissue. In three of the four tissues tested, a very weak signal for KCNQ5 was also observed. This profile was similar to that described by Ohya *et al*. (2003) by quantitative PCR, that is, KCNQ1 ≫ KCNQ4 > KCNQ5 > KCNQ3. Amplicons for KCNQ1, KCNQ4 and KCNQ5 were also detected in RNA samples isolated from a pool of 20 single myocytes using a nested RT-PCR approach (Figure 7aii). To consolidate the PCR results, immunocytochemical imaging using antibodies against different KCNQ expression products ($K_v7.x$) was undertaken. Figure 7bi shows positive staining for $K_v7.1$ ($n=6$ cells), $K_v7.4$ (Kv7.4J, $n=6$ cells, panel 7ci; $K_v7.4$SC, $n=6$ cells, panel 7di). Figure 7bi shows positive staining for $K_v7.1$ ($n=6$ cells), panel 7ci the staining for $K_v7.4$ (Kv7.4J, $n=6$ cells) and in panel 7di, staining for $K_v7.4$SC ($n=6$ cells). The fluorescent signal for both $K_v7.1$ and $K_v7.4$ subunits were located predominantly within 1 μm of the plasma membrane, with significantly less signal originating in the cytoplasm (Figure 7e). Pre-incubation of the $K_v7.1$ antibody with its antigenic peptide (1:2 ratio of antibody to antigenic peptide) suppressed the fluorescence strongly (compare panel 7bi to panel 7bii; summary in Figure 7f, $n=4$–6, $P<0.001$; unpaired Student's *t*-test). Incubation of the $K_v7.4$SC antibody with its antigenic peptide also produced a significant reduction in the

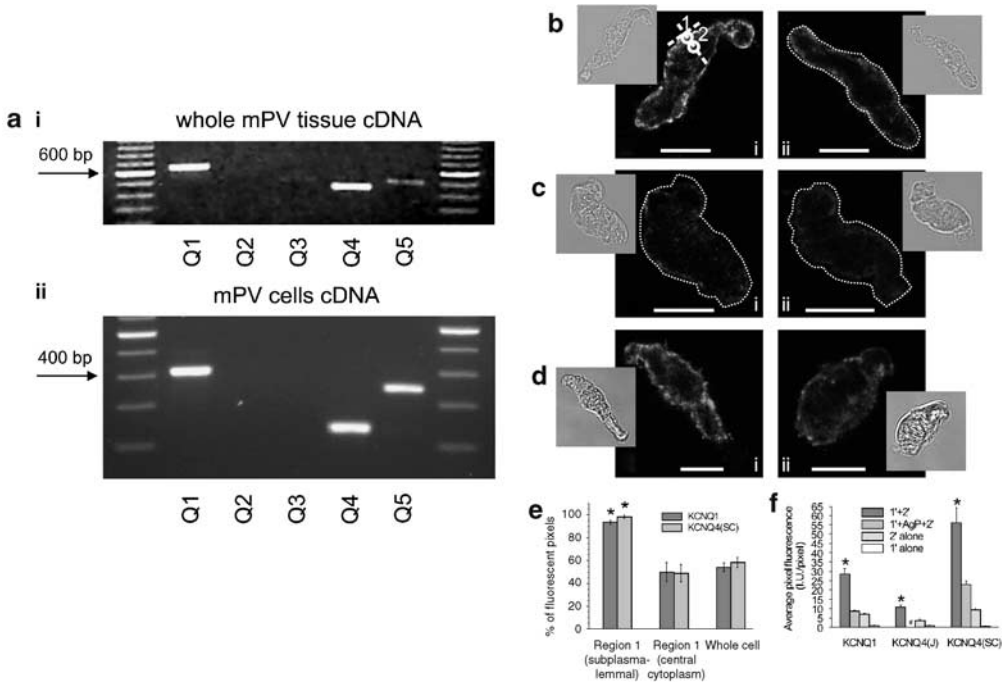

Figure 7 Expression of mRNA and protein in mPV tissue and cells. (**a**) RT-PCR analysis of KCNQ genes in RNA extracted from mPV tissue (**i**) or a pool of 20 isolated myocytes (**ii**). In panel **7aii**, the size of the products are different from those in **7ai** because a nested PCR was used. Immunocytochemical staining of murine portal vein myocytes for (**b**) $K_v7.1$ and (**c** and **d**) $K_v7.4$. The right-hand panels show control experiments in the presence of an antigenic peptide (**b** and **d**) or in the absence of primary antibodies (**c**). White circles in panel *bi* indicate Regions 1 and 2, which were used to analyse the localization of fluorescence. A dotted line was used where necessary to outline the contour of a cell, due to its low fluorescence. The insets show transmitted light images of respective cells. Calibration: 10 μm. (**e**) Summarized data on localization of K_v7 fluorescence in the cells showing the percentage of fluorescent pixels in the region within ~1 μm of plasma membrane (Region 1), in the deep cytoplasm (Region 2) and in the whole confocal plane. (**f**) Summary data showing the specificity of labelling, confirmed by a significant decrease in fluorescence either after preincubation with antigenic peptide (AgP) or in the absence of primary antibodies. 1′ = Region1; 2′ = Region 2 *Significantly different from other values shown. #: antigenic peptide not available.

fluorescence intensity (compare panel 7di to panel 7dii; summary in Figure 7f, $n = 4$–6, $P < 0.05$; unpaired Student's *t*-test,) although complete suppression was not observed. Similar to the $K_v7.4$SC antibody, the immunofluorescent signal of the $K_v7.4$J, although weak, was found predominantly within 1 μm of the plasma membrane. These data confirm that $K_v7.1$, and $K_v7.4$ proteins are present in the cell membrane of mPV myocytes, as described recently in murine thoracic aorta (Yeung *et al*., 2007).

Effect of retigabine on heterologously expressed KCNQ channels

Given the bimodal effects of retigabine and flupirtine on endogenous K^+ currents, we compared the effect of retigabine and flupirtine on KCNQ1, KCNQ4 and KCNQ5 heterologously expressed as homomers in *Xenopus* oocytes (Figure 8). KCNQ1 was unaffected by either retigabine or flupirtine (data not shown) whereas both KCNQ4 and KCNQ5 were augmented by retigabine (Figures 8a–h) and flupirtine (Figures 8i–l). A mean increase in currents was observed with retigabine for KCNQ4 (Figure 8c) and KCNQ5 (Figure 8g) starting at −60 mV and flupirtine (KCNQ4—Figure 8i; KCNQ5—Figure 8k) starting at −40 mV. None of the oocytes analysed, which expressed either KCNQ4 or KCNQ5, showed an inhibition at more positive potentials.

Discussion

Retigabine and its close structural analogue flupirtine augment native K^+ channels in a number of neuronal types including cortical neurones (Rundfeldt, 1997), superior cervical ganglia (Tatulian *et al*., 2001) and visceral sensory neurones (Wladyka and Kunze, 2006). The subsequent suppression of neuronal electrical activity underpins the development of retigabine as an anti-epileptic agent (Porter *et al*., 2007). The present study showed that retigabine and flupirtine also stimulated native K^+ channel currents in mPV myocytes, hyperpolarized the resting membrane potential and markedly inhibited the spontaneous contractility of the whole portal vein. This study therefore, represents the first direct illustration of retigabine modulating K^+ channels in a non-neuronal cell type.

The current enhancement produced by retigabine was suppressed completely by the KCNQ channel blocker XE991 (10 μM) confirming that the observed effects were mediated by the stimulation of K_v7 channels in these myocytes. In addition, the present work describes, in full, a bimodal effect of retigabine and flupirtine on native K^+ channels, as currents at potentials positive to ~0 mV were decreased by these agents. Again this effect was prevented by pre-incubation of the cells with XE991 suggesting that the native K_v7 channel complexes have both stimulatory and

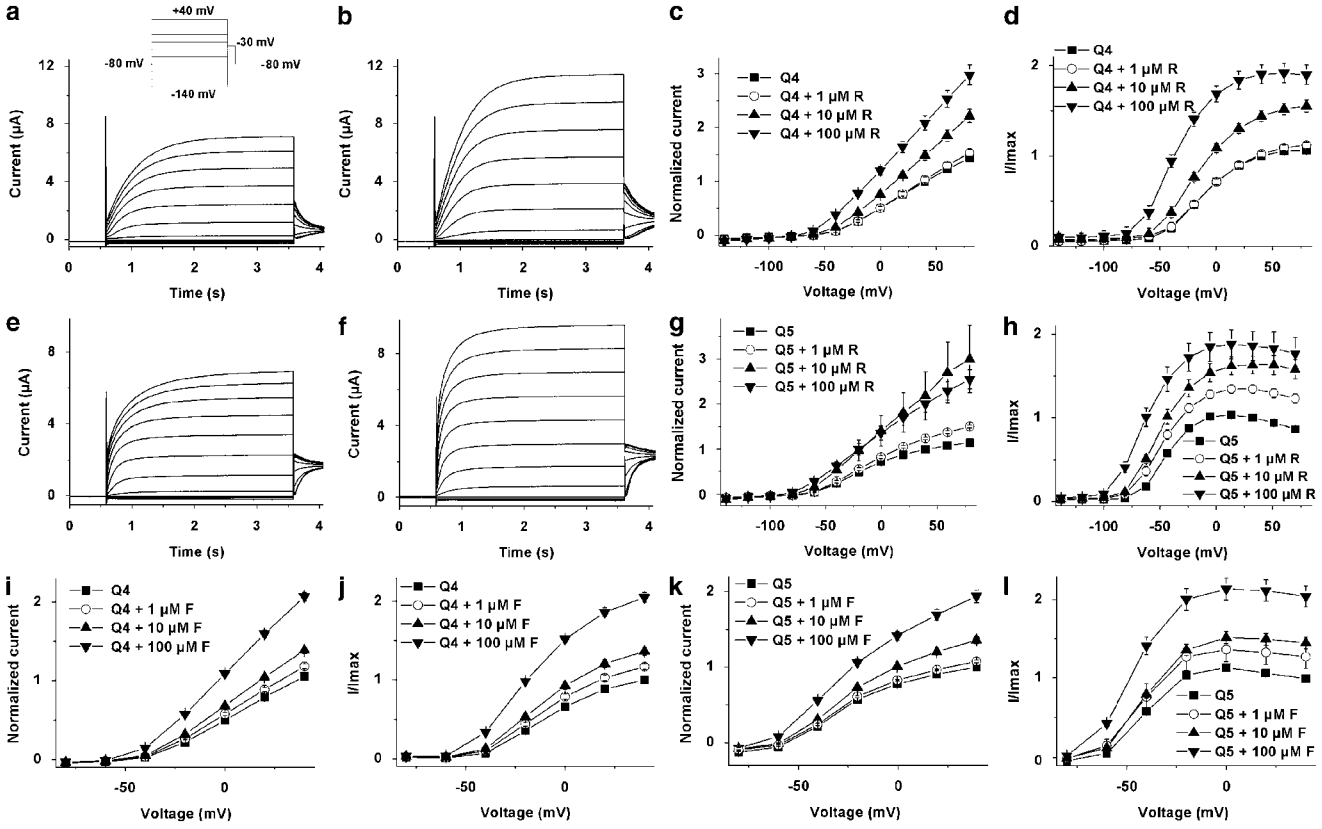

Figure 8 Activation of heterologously expressed KCNQ4 and KCNQ5 by retigabine and flupirtine. Typical current traces of oocytes expressing KCNQ4 (**a**) and KCNQ5 (**e**) before and after (KCNQ4 (**b**); KCNQ5 (**f**)) the application of 10 μM retigabine (R). The voltage protocol used for these experiments is shown as inset in panel a. I/V curves of KCNQ4 (**c** and **i**) and KCNQ5 (**g** and **k**) as a summary of the current recordings, which were obtained from oocytes measured with different retigabine (KCNQ4 (**c**) and KCNQ5 (**g**)) and different flupirtine (F) concentrations (KCNQ4 (**i**) and KCNQ5 (**k**)). I/I_{max} curves of KCNQ4 and KCNQ5 as a function of voltage obtained from tail current analysis and different retigabine (KCNQ4 (**d**) and KCNQ5 (**h**)) or flupirtine (KCNQ4 (**j**) and KCNQ5 (**l**)) concentrations. For all experiments n=8.

inhibitory sites. This bimodal effect has been mentioned briefly in previous papers using studies on neuronal cells. Both Rundfeldt (1997) and Tatulian *et al*. (2001) reported that the retigabine-sensitive current plotted against test potential had a distinctive 'bell' shape but did not describe a net inhibition. This is probably because the voltage range in these studies was truncated at 0 mV, whereas, in the present study, a net inhibition was only manifest with the highest concentration used (20 μM). In contrast to the bimodal effect on native K^+ currents in mPV myocytes, retigabine or flupirtine simply augmented K^+ currents produced by the overexpression of KCNQ 4 or 5 in *Xenopus* oocytes. Neither compound affected currents produced by the overexpression of KCNQ1. This is a highly pertinent observation because it suggests that simple K_v7 homomers do not constitute the native channel in mPV myocytes. It is possible that the native channel is formed from heteromers of $K_v7.1$, 7.4 or 7.5, as the mPV myocytes express KCNQ1, 4 and 5. However, all past reports that analyzed *Xenopus* oocytes coexpressing these Kv7 subunits, have so far failed to show an interaction of these channels (Kubisch *et al*., 1999; Jentsch, 2000; Schroeder *et al*., 2000). Consequently, the bimodal phenomenon represents an interesting finger-print of the native vascular K_v7 channels.

The molecular targets of retigabine are the so-called 'neuronal' K_v7 channels, that is, those encoded by the genes KCNQ2–5 (Main *et al*., 2000; Wickenden *et al*., 2000; Tatulian *et al*., 2001). Retigabine augments currents generated by KCNQ2/3 hetero-multimers and KCNQ5/3 hetero-multimers with an EC_{50} of 0.3–2 μM (Wickenden *et al*., 2000, 2001; Tatulian *et al*., 2001, present study). Retigabine has a similar concentration dependence for currents generated by the overexpression of KCNQ3 (1 μM, Tatulian *et al*., 2001), and KCNQ4 (5 μM, Tatulian *et al*., 2001, present study). The stimulatory effect is due mainly to a 20–40 mV leftward shift in the voltage-dependence of activation, dependent on the KCNQ isoform (Main *et al*., 2000; Wickenden *et al*., 2000; Tatulian *et al*., 2001) although KCNQ5-encoded channels are augmented without an effect on the half-activation voltage (Dupuis *et al*., 2002). Interestingly, retigabine produced a modest shift (~10 mV) of current activation in mPV myocytes. Retigabine also speeds the rate of activation and slows deactivation (Main *et al*., 2000). No inhibition of channels encoded by KCNQ2–5 has ever been reported and was not observed in the present study. In stark contrast to the stimulatory effect on channels encoded by KCNQ2–5, retigabine in concentrations up to 100 μM does not increase KCNQ1-generated currents (Tatulian *et al*., 2001; Schenzer *et al*., 2005; Wuttke *et al*., 2005). In fact, currents generated

by the heterologous expression of KCNQ1 are inhibited in a voltage-dependent manner by retigabine with an IC_{50} of $\sim 100\,\mu M$ (Tatulian *et al*., 2001). This led to the identification of tryptophan 236 in the S5 domain and glycine301 in the S6 domain of KCNQ2–5 as crucial amino acids for the stimulatory effect of retigabine (Schenzer *et al*., 2005; Wuttke *et al*., 2005). With respect to the opposing effect of retigabine on channels encoded by KCNQ1 versus other KCNQ genes, the bimodal effect observed in mPV myocytes may reflect differential effects on K_v7 channels. Thus, at negative potentials, activation of $K_v7.4/K_v7.5$ by retigabine dominates leading to current augmentation but at positive potentials, block of $K_v7.1$ dominates resulting in the observed current inhibition. However, the inability of chromanol 293B to prevent the retigabine-induced current inhibition at $+40\,mV$ suggests that this model needs to be investigated further.

KCNQ expression in smooth muscle cells

KCNQ gene expression in smooth muscle cells was first identified in rat stomach by Ohya *et al*. (2002a). This observation was followed by an in-depth study in mPV where both KCNQ and KCNE gene expression was quantified (Ohya *et al*., 2002b, 2003). We have now extended these observations to include the murine aorta and a number of different conduit arteries (carotid, femoral and mesenteric, Yeung *et al*., 2007). In every case the most abundantly expressed genes were KCNQ1 and KCNQ4, the latter hitherto considered to be only expressed in auditory nerves (Kharkovets *et al*., 2000; Kubisch *et al*., 1999). Some KCNQ5 expression was also detected whereas KCNQ2 and 3 were conspicuous by their absence (see Ohya *et al*., 2003; Brueggemann *et al*., 2006; Yeung *et al*., 2007). The previous study on mPV showed that KCNQ1 was the most abundantly expressed with KCNQ4 having significant abundance (Ohya *et al*., 2003). We have now consolidated these findings and shown that $K_v7.4$ protein is present in the plasmalemmal membrane of portal vein myocytes as well as $K_v7.1$, similar to the situation in murine aortic myocytes (Yeung *et al*., 2007).

Previous studies on mPV showed that the selective KCNQ channel blocker XE991, which does not discriminate between different K_v7 isoforms, inhibited K^+ currents, depolarized the membrane potential and increased spontaneous contractions consistent with K_v7 channels regulating cellular excitability (Yeung and Greenwood, 2005). XE991 also contracts segments of aorta (Yeung *et al*., 2007), as well as conduit arteries such as the pulmonary (Joshi *et al*., 2006), carotid and femoral (Yeung *et al*., 2007). These observations were consistent with K_v7 channels regulating the membrane potential and suppressing voltage-dependent Ca^{2+} influx in smooth muscle cells throughout the vasculature. Moreover, it is probably not $K_v7.1$ subunits that are important for this effect but $K_v7.4$ or $K_v7.5$ as $K_v7.1$-selective blockers (chromanol 293B or L-768, 673) failed to mirror the effects of XE991 (Yeung *et al*., 2007). This postulate was supported by the ability of retigabine (2–20 μM) to relax segments of aorta, as well as carotid, femoral and mesenteric arteries precontracted with phenylephrine, but not with raised external K^+ (Yeung *et al*., 2007). The electrophysiological and mechanical effects obtained in the present study agree with the hypothesis that $K_v7.4$ or $K_v7.5$ channels are key regulators of vascular excitability. However, as mentioned above, the bimodal effects of retigabine and flupirtine argue against simple K_v7 homomers existing in vascular myocytes. Vascular myocytes do express various members of the KCNE gene family, (Ohya *et al*., 2002a; Yeung *et al*., 2007), which are known to influence the biophysical and pharmacological attributes of K_v7 channels (for example, Grunnet *et al*., 2002; Strutz-Seebohm *et al*., 2006). Consequently, the native 'KCNQ channel' in vascular smooth muscle cells may result from a hitherto undefined combination of KCNQ and KCNE gene products. Future studies will investigate this aspect further.

To conclude, we have shown that retigabine and flupirtine activate K^+ channels and this mechanism underlies the vasorelaxant effect of these agents reported previously (Yeung *et al*., 2007). In addition, both agents inhibit XE991-sensitive currents at positive potentials and this phenomenon provides an interesting signature in future studies aimed at deciphering the molecular identity of the native K_v7 channel in smooth muscle cells.

Acknowledgements

Research in Dr Greenwood's laboratory was funded by the British Heart Foundation (PG/O3/085/15747). This research was also supported by Deutsche Forschungsgemeinschaft (MS) and a British Heart Foundation Intermediate Research Fellowship FS/04/052 (VP). We are grateful to Professor Thomas Bolton for the access to the confocal microscope.

Conflict of interest

The authors state no conflict of interest.

References

Alexander SPH, Mathie A, Peters JA (2008). Guide to Receptors and Channels (GRAC), 3rd edn. *Br J Pharmacol* **153** (Suppl. 2): S1–S209.

Brueggemann LI, Moran CJ, Barakat JA, Yehy JZ, Cribbs LL, Byron KL (2006). Vasopressin stimulates action potential firing by protein kinase C dependent inhibition of KCNQ5 in A7r5 rat aortic smooth muscle cells. *Am J Physiol-Heart* **292**: H1352–H1363.

Dupuis DS, Olesen S-P, Jespersen T, Christensen JK, Christophersen P, Jensen BS (2002). Activation of KCNQ5 Channels stably expressed in HEK293 cells by BMS-204352. *Eur J Pharmacol* **437**: 129–137.

Grunnet M, Jespersen T, Rasmussen HB, Ljungstrom T, Jorgensen NK, Olesen SP *et al*. (2002). KCNE4 is an inhibitory subunit to the KCNQ1 channel. *J Physiol* **542**: 119–130.

Jentsch TJ (2000). Neuronal KCNQ potassium channels: physiology and role in disease. *Nat Rev Neurosci* **1**: 21–30.

Joshi S, Balan P, Gurney AM (2006). Pulmonary vasoconstrictor action of KCNQ potassium channel blockers. *Respir Res* **7**: 31.

Kharkovets T, Hardelin JP, Safieddine S, Schweizer M, El-Amraoui A, Petit C *et al*. (2000). KCNQ4, a K^+ channel mutated in a form of dominant deafness, is expressed in the inner ear and the central auditory pathway. *Proc Natl Acad Sci USA* **97**: 4333–4338.

Kubisch C, Schroeder BC, Friedrich T, Luetjohann B, El-Amraoui A, Marlin S *et al*. (1999). KCNQ4, a novel potassium channel

expressed in sensory outer hair cells, is mutated in dominant deafness. *Cell* **96**: 437–446.

Lerche C, Bruhova I, Lerche H, Steinmeyer K, Wei AD, Strutz-Seebohm N *et al*. (2007). Chromanol 293B binding in KCNQ1 (Kv7.1) channels involves electrostatic interactions with a potassium ion in the selectivity filter. *Mol Pharmacol* **71**: 1503–1511.

Main MJ, Cryan JE, Dupere JR, Cox B, Clare JJ, Burbidge SA (2000). Modulation of KCNQ2/3 potassium channels by the novel anticonvulsant retigabine. *Mol Pharmacol* **58**: 253–262.

Ohya S, Asakura K, Muraki K, Watanabe M, Imaizumi Y (2002b). Molecular and functional expression of ERG, KCNQ, and KCNE subtypes in rat stomach smooth muscle. *Am J Physiol (Gastro Liv Physiol)* **282**: 277–287.

Ohya S, Horowitz B, Greenwood IA (2002a). Functional and molecular identification of ERG channels in murine portal vein myocytes. *Am J Physiol Cell Physiol* **283**: C866–C877.

Ohya S, Sergeant G, Greenwood IA, Horowitz B (2003). Molecular variants of KCNQ channels expressed in murine portal vein myocytes: a role in delayed rectifier current. *Circ Res* **92**: 1016–1023.

Porter RJ, Nohria V, Rundfeldt C (2007). Retigabine. *Neurotherapeutics* **4**: 149–154.

Rundfeldt C (1997). The new anticonvulsant retigabine (D-23129) acts as an opener of K^+ channels in neuronal cells. *Eur J Pharmacol* **336**: 243–249.

Saleh S, Yeung SY, Prestwich S, Pucovsky V, Greenwood IA (2005). Electrophysiological and molecular identification of voltage-gated sodium channels in murine vascular myocytes. *J Physiol* **568**: 155–169.

Schenzer A, Friedrich T, Pusch M, Saftig P, Jentsch TJ, Grötzinger J *et al*. (2005). Molecular determinants of KCNQ (Kv7) K^+ channel sensitivity to the anticonvulsant retigabine. *J Neurosci* **25**: 5051–5060.

Schroeder BC, Hechenberger M, Weinrich F, Kubisch C, Jentsch TJ (2000). KCNQ5, a novel channel broadly expressed in brain, mediates M-current. *J Biol Chem* **275**: 24089–24095.

Strutz-Seebohm N, Seebohm G, Fedorenko O, Baltaev R, Engel J, Knirsch M *et al*. (2006). Functional coassembly of KCNQ4 with KCNE-beta-subunits in *Xenopus* oocytes. *Cell Physiol Biochem* **18**: 57–66.

Tatulian L, Delmas P, Abogadie FC, Brown DA (2001). Activation of expressed KCNQ potassium currents and native neuronal M-type potassium currents by the anti-convulsant drug retigabine. *J Neurosci* **21**: 5535–5545.

Wang H-S, Brown BS, McKinnon D, Cohen IR (2000). Molecular basis for differential sensitivity of KCNQ and I_{Ks} channels to the cognitive enhancer XE991. *Mol Pharmacol* **57**: 1218–1223.

Wang H-S, Pan Z, Shi W, Barry BS, Wymore RS, Cohen IR *et al*. (1998). KCNQ2 and KCNQ3 potassium channel subunits: molecular correlates of the M-channel. *Science* **282**: 1890–1893.

Wickenden AD, Yu W, Zou A, Jegla T, Wagoner PK (2000). Retigabine, a novel anti-convulsant, enhances activation of KCNQ2/Q3 potassium channels. *Mol Pharmacol* **58**: 591–600.

Wickenden AD, Zou A, Wagoner PK, Jegla T (2001). Characterization of KCNQ5/Q3 potassium channels expressed in mammalian cells. *Br J Pharmacol* **132**: 381–384.

Wladyka CL, Kunze DL (2006). KCNQ/M-currents contribute to the resting membrane potential in rat visceral sensory neurones. *J Physiol* **575**: 175–189.

Wuttke TV, Seebohm G, Bail S, Maljevic S, Lerche H (2005). The new anticonvulsant retigabine favors voltage-dependent opening of the Kv7.2 (KCNQ2) channel by binding to its activation gate. *Mol Pharmacol* **67**: 1009–1017.

Yeung SYM, Greenwood IA (2005). Electrophysiological and functional effects of the KCNQ channel blocker XE991 on murine portal vein smooth muscle cells. *Br J Pharmacol* **146**: 585–595.

Yeung SYM, Pucovský V, Moffatt JD, Saldanha L, Schwake M, Ohya S *et al*. (2007). Molecular expression and pharmacological identification of a role for K_v7 channels in murine vascular reactivity. *Br J Pharmacol* **151**: 758–770.